HHS Public Access

Author manuscript

Cell Rep. Author manuscript; available in PMC 2021 August 25.

Published in final edited form as:

Cell Rep. 2021 August 03; 36(5): 109469. doi:10.1016/j.celrep.2021.109469.

Nucleus basalis stimulation enhances working memory by stabilizing stimulus representations in primate prefrontal cortical activity

Xue-Lian Qi[1], **Ruifeng Liu**[2,3], **Balbir Singh**[1,4], **David Bestue**[5], **Albert Compte**[5], **Almira I. Vazdarjanova**[6,7], **David T. Blake**[2], **Christos Constantinidis**[1,4,8,9,10,*]

[1]Department of Neurobiology & Anatomy, Wake Forest School of Medicine, Winston-Salem, NC 27157, USA

[2]Department of Neuroscience and Regenerative Medicine, Medical College of Georgia, Augusta University, Augusta, GA 30912, USA

[3]State Key Laboratory of Ophthalmology, Zhongshan Ophthalmic Center, Sun Yat-sen University, Guangzhou, China

[4]Department of Biomedical Engineering, Vanderbilt University, Nashville, TN 37235, USA

[5]Institut d'Investigacions Biomèdiques August Pi i Sunyer (IDIBAPS), Barcelona, Spain

[6]Charlie Norwood VA Medical Center, Augusta, GA, USA

[7]Department of Pharmacology & Toxicology, MCG, Augusta University, Augusta, GA 30912, USA

[8]Neuroscience Program, Vanderbilt University, Nashville, TN 37235, USA

[9]Department of Ophthalmology and Visual Sciences, Vanderbilt University Medical Center, Nashville, TN 37232, USA

[10]Lead contact

SUMMARY

Acetylcholine plays a critical role in the neocortex. Cholinergic agonists and acetylcholinesterase inhibitors can enhance cognitive functioning, as does intermittent electrical stimulation of the cortical source of acetylcholine, the nucleus basalis (NB) of Meynert. Here we show in two male monkeys how NB stimulation affects working memory and alters its neural code. NB stimulation increases dorsolateral prefrontal activity during the delay period of spatial working memory tasks and broadens selectivity for stimuli but does not strengthen phasic responses to each neuron's

* **Correspondence:** christos.constantinidis.1@vanderbilt.edu .

AUTHOR CONTRIBUTIONS

C.C. and D.T.B. designed the experiments. R.L., C.C., X.-L.Q., and D.T.B. performed surgeries. X.-L.Q. and C.C. conducted behavioral and neurophysiological experiments. X.-L.Q., B.S., D.B., A.C., and C.C. performed data analysis. A.I.V. conducted immunohistochemistry experiments. C.C., X.-L.Q., and D.T.B. wrote the manuscript, with input from all authors.

DECLARATION OF INTERESTS

The authors declare no competing interests.

SUPPLEMENTAL INFORMATION

Supplemental information can be found online athttps://doi.org/10.1016/j.celrep.2021.109469.

optimal visual stimulus. Paradoxically, despite this decrease in neuronal selectivity, performance improves in many task conditions, likely indicating increased delay period stability. Performance under NB stimulation does decline if distractors similar to the target are presented, consistent with reduced prefrontal selectivity. Our results indicate that stimulation of the cholinergic forebrain increases prefrontal neural activity, and this neuromodulatory tone can improve cognitive performance, subject to a stability-accuracy tradeoff.

Graphical abstract

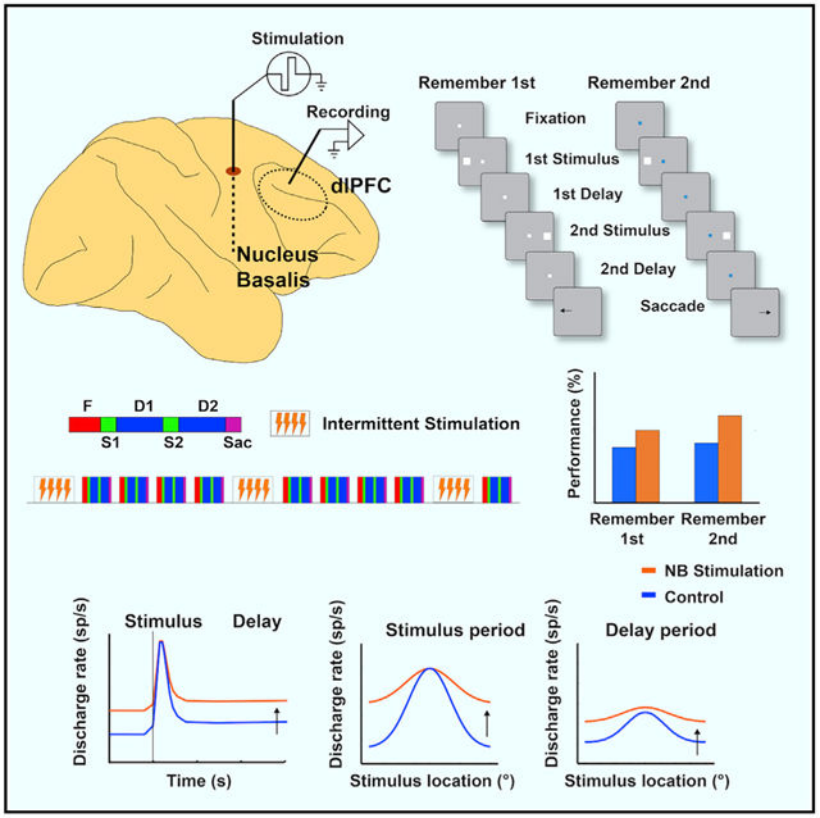

In brief

Qi et al. show that intermittent electrical stimulation of the nucleus basalis of Meynert, the source of cholinergic innervation of the cerebral cortex, improves performance in working memory tasks. NB stimulation increases activity of dorsolateral prefrontal neurons and broadens tuning, making the network that maintains information in memory more stable.

INTRODUCTION

The forebrain cholinergic system tightly regulates higher cognitive function (Galvin et al., 2018; Sarter et al., 2016). Losses in cognitive performance with aging and Alzheimer's disease occur in parallel with degeneration of the brain's cholinergic systems, and cholinergic deficits correlate tightly with the degree of cognitive decline (Ballinger et al.,

2016; Terry and Buccafusco, 2003). Cholinesterase inhibitors are frontline medications in Alzheimer's disease (Birks and Harvey, 2018).

Improvement in cognitive functions may alternatively be achieved by stimulation of the nucleus basalis (NB) of Meynert (Freund et al., 2009), the source of neocortical acetylcholine in humans and other primates (Mesulam et al., 1983). This approach offers distinct benefits over drug administration, including avoidance of peripheral cholinergic stimulation, optimized timing, and activation of non-cholinergic projection neurons, which are normally co-active with the cholinergic fibers (Kim et al., 2015; Walker et al., 1989). Stimulation of basal forebrain neurons is effective in the context of neuroplasticity (Bakin and Weinberger, 1996; Brzosko et al., 2019; Froemke, 2015; Kilgard and Merzenich, 1998) and in enhancing behavioral performance of attention and memory tasks, with improvements that aggregate rather than attenuate over time (Blake et al., 2017; Liu et al., 2017, 2018).

We were therefore motivated to examine how intermittent NB stimulation affects neuronal activity to improve performance of working memory tasks. We focused specifically on the prefrontal cortex (PFC), an area critical for working memory and cognitive plasticity (Constantinidis and Klingberg, 2016), which receives innervation from a rostral cluster of NB neurons (Gielow and Zaborszky, 2017; Mesulam et al., 1983; Yuan et al., 2019).

RESULTS

Two monkeys were implanted with unilateral electrodes targeting the NB to determine the effects of stimulation on behavioral performance and neural activity. Electrode placement was guided by magnetic resonance (MR) imaging (Figure 1A). To obtain functional confirmation of the targeting, we collected local field potential (LFP) signals from the implanted electrode with the monkey at rest, with and without NB stimulation (Bjordahl et al., 1998). Continuous NB stimulation at 80 Hz produced LFP desynchronization (Figure 1B). Power in the 5–15 Hz range was significantly lower during NB stimulation than control (paired t test, $t_{17} = 3.14$, $p = 0.006$ and $t_{33} = 2.5$, $p = 0.02$ for the two subjects, respectively). Electrode placement was confirmed with choline acetyltransferase (ChAT) immunohisto-chemistry, which identifies acetylcholine-producing neurons, post mortem (Figures 1C-1E). Control sections where the primary antibody was omitted produced no distinct cell-specific staining.

Behavioral performance

The monkeys performed a task requiring them to view two stimuli presented in sequence and make an eye movement to the remembered location of either the first or second depending on the color of the fixation point (white or blue, respectively; Figure 2A). The stimuli could appear at any of eight possible locations, presented in a randomized order (see insets in Figures S1 and S2). When NB stimulation was delivered, it was applied during an inter-trial interval between two trials for 15 s, at a frequency of 80 pulses/s (Figures 2B-2D). The monkeys performed consecutive trials for 45 s (typically 4–5 completed trials), without NB stimulation. At the end of the trial that exceeds the 45-s threshold, NB stimulation was applied anew and the cycle was repeated.

NB stimulation was delivered in two modes. In the first mode, daily sessions were performed without any NB stimulation, and these were preceded or followed by daily sessions during which intermittent NB stimulation was performed based on the schedule indicated in Figure 2C. These daily sessions allowed us to collect a large number of trials and characterize the behavioral performance of the monkeys (Figures 2E-2H). In the second mode, when neuronal recordings commenced, the monkeys performed blocks of 60 trials without NB stimulation, followed by blocks of trials with NB stimulation, which in this case, too, was applied in intermittent fashion, during the inter-trial interval of stimulation blocks.

Behavioral performance generally improved with intermittent NB stimulation delivered in daily sessions over sessions without stimulation (Figures 2E-2H). For monkey GR, improvement was observed for both ipsilateral and contralateral conditions. A three-way ANOVA for this monkey's performance with factors (1) NB stimulation (on or off), in a between-sessions design; (2) task (remember-first or remember-second); and (3) location of visual stimuli (contralateral or ipsilateral visual stimulus to be remembered) revealed a significant main effect of NB stimulation ($F_{1,128} = 19.6$, $p = 2.06 \times 10^{-5}$). For monkey HE, stimulation improved performance specifically when the visual stimulus to be remembered was at a location contralateral to the site of the stimulation electrode (Figures 2E-2G). NB stimulation led to decreased performance when the visual stimulus was ipsilateral to the stimulation (Figures 2F and 2H). Performing the same three-way ANOVA analysis showed a significant three-way interaction between task, stimulation, and side of visual stimulus ($F_{1,128} = 6.04$, $p = 0.015$). Considering the contralateral conditions alone (Figures 2E-2G), the effect of NB stimulation was highly significant (three-way ANOVA with factors monkey and stimulation: $F_{1,173} = 14.14$, $p = 0.0002$ for remember-first task; $F_{1,173} = 5.61$, $p = 0.02$ for remember-second task). Dissecting the effect of stimulation for different combinations of stimulus locations additionally revealed that performance for visual stimuli appearing at adjacent locations was lower under NB stimulation than control (two-tailed t test, $t_{66} = 2.83$, $p = 0.006$) in the remember-first (Figure 2I, 45° distance), but not the remember-second condition (Figure 2J), with excess errors directed to the location of the distractor.

Overall effects on neural activity

We recorded from a total of 233 neurons in areas 8 and 46 of the dorsolateral PFC (102 and 131 neurons in the two monkeys, respectively). Recordings were obtained first under control conditions and then under NB stimulation, always delivered in the inter-trial interval. Recording cylinders were implanted on the same side as the stimulation electrode. NB stimulation had a predominantly excitatory effect in neural activity recorded in correct trials (Figures 3A-3D). Mean firing rate averaged across all neurons (Figure 3E) during the fixation period was 10.9 spikes/s (sp/s) in control trials and 13.4 sp/s in NB stimulation trials, a significant difference (two-tailed paired t test, $t_{232} = 4.21$, $p = 3.65 \times 10^{-5}$). During the visual stimulus presentation period, mean firing rate (averaged across all visual stimulus conditions and neurons) was 13.4 sp/s for the control and 16.2 sp/s for the NB stimulation condition (two-tailed paired t test, $t_{232} = 4.39$, $p = 1.7 \times 10^{-5}$). A similar trend was observed in both monkeys (13.4 versus 16.0 sp/s, $p = 9.5 \times 10^{-5}$; 13.3 versus 16.3 sp/ s, $p = 0.023$ for the two animals, respectively). However, the increase in firing rate

was not uniform across stimuli; it was accounted mostly by increased responsiveness to suboptimal stimuli, rather than the best stimulus of each neuron, which remained relatively unchanged. The effects of NB stimulation were not uniform across neurons, either. NB stimulation produced a significant increase in fixation period firing rate for 97/233 neurons (estimated with a t test, at the 0.05 significance level), no significant difference in 99/233 neurons, but also a decrease in firing rate for 37/233 of neurons. The distribution of firing rate differences computed in blocks of trials with or without NB stimulation deviated significantly from a normal distribution (Kolmogorov-Smirnov [KS] test for normalized rate differences, compared with normal distribution, $p = 8.74 \times 10^{-6}$).

NB stimulation did not only affect firing rates but also their variability. A significant decrease in Fano factor, a measure of trial-to-trial variability, was observed under NB stimulation (Figure 3G). The reduction over the control condition was evident in all task intervals. A two-way ANOVA, with factors task-interval and stimulation, showed a significant main effect of stimulation ($F_{1,1353} = 10.1$, $p = 0.0015$) but no interaction ($F_{2,1353} = 0.17$, $p = 0.8$).

Effects in different task intervals

Among neurons recorded, 112 (67 and 45 from the two subjects, respectively) responded to the visual stimuli (evaluated with a paired t test, at the $p < 0.05$ significance level during the visual stimulus presentation or delay period). We examined these neurons in more detail, because they were revealing of the effects of NB stimulation in the context of the task. For a total of 54 neurons that responded to visual stimuli (41 and 13 from subjects GR and HE, respectively), firing rate in the fixation period was significantly higher after NB stimulation (evaluated with a t test at the $p < 0.05$ level; as in Figures 3A-3D). For 16 neurons, firing rate was significantly decreased.

For the neurons with an overall increase in activation during the fixation interval (Figure 4), the effect was stable over the time course of ~1 min between cycles of repeated stimulation (see Figures 2B and 2C). The firing rate was elevated in the first trial following stimulation, and no decrease was evident in the 4–5 successive trials that followed until the next train of stimulation was applied (Figure 4H, red line). Interestingly, NB stimulation did not produce uniform effects across all task intervals. In the same group of neurons, NB stimulation had no effect during the inter-trial interval (Figure 4A, two-way ANOVA with factors tasks and stimulation: main effect of stimulation $F_{1,53} = 2.6$, $p = 0.113$). The phasic response to the preferred visual stimulus itself (peak in ~200 ms after visual stimulus) was also largely unchanged between the control and NB stimulation conditions (Figure 4A, two-way ANOVA with factors tasks and stimulation: main effect of stimulation $F_{1,53} = 0.397$; $p = 0.53$). The absence of an enhancement to the preferred visual stimulus response was evident in both the remember-first and remember-second tasks (Figures S1 and S2) and for both the first and second presentation of a visual stimulus in the receptive field (Figure 4A). In contrast, the increase in firing rate in trials with NB stimulation persisted during the delay periods after each stimulus presentation (two-way ANOVA with factors tasks and stimulation: main effect of stimulation $F_{1,53} = 6.20$, $p = 0.016$ for first delay period; $F_{1,53} = 6.42$, $p = 0.014$ for second delay period). These results of NB stimulation moved in the same

direction for both remember-first and remember-second tasks and for both monkeys (Figures S3A and S3B).

Neural tuning

NB stimulation did not increase responses following the best visual stimulus but instead enhanced responses to visual stimuli at non-optimal locations, which resulted in broadening of receptive fields during the cue presentation and delay period (second visual stimulus in Figures 4C-4E; first visual stimulus in Figures S1F-S1J). The broadening of the receptive fields was also evident in the remember-second task (Figures S2F-S2J). The population tuning curve based on the second-visual stimulus location illustrated the effect (Figure 4I). To quantify differences in responsiveness to sub-optimal visual stimuli on a neuron-by-neuron basis, we relied on a selectivity index (SI) defined as (Max − Min)/(Max + Min), where Max and Min represent the firing rate to the best and worst stimulus location for each neuron (Figures S4A-S4D). NB stimulation produced a significantly lower SI value (two-way ANOVA with factors remember-first/remember-second tasks and stimulation: main effect of stimulation $F_{1,53} = 25.4$, $p = 5.7 \times 10^{-6}$ for cue period, and $F_{1,53} = 24.2$, $p = 8.7 \times 10^{-6}$ for delay period). Other measures of selectivity, such as the receiver operating characteristic (Figures S4E-S4H) and percentage of explained variance, revealed similar effects (Figures S4I-S4J). Unlike the decrease in selectivity for visual stimulus location in prefrontal neuronal activity, however, the representation of task information (higher firing rate for remember-first or remember-second) was relatively unaffected by NB stimulation (Figure S4K).

NB stimulation in the remember-second task yielded another unexpected finding: responses in anticipation of a visual stimulus, even when none was presented (Figures 4F and 4G). Our behavioral task involved a fixed duration of the fixation interval that the monkey could time. A visual stimulus was most often presented after this interval; however, in 20% of the trials, no visual stimulus was presented, and the trial continued with the presentation of the ‘‘second’’ visual stimulus at its expected time (see insets in Figures 4F and 4G). NB stimulation elicited elevated firing rate in the time interval that the first visual stimulus would have been expected in no-visual stimulus trials (two-way ANOVA with factors tasks and stimulation: main effect of stimulation $F_{1,53} = 26.9$, $p = 3.4 \times 10^{-6}$). Such an anticipatory signal was absent without NB stimulation, although presumably the monkey was anticipating a visual stimulus in these trials, too (Figures 4F and 4G).

NB stimulation effects beyond increased firing rate

Neurons that responded to visual stimuli but for which stimulation produced decreased activity (n = 16; 7 and 9 from monkeys GR and HE, respectively) were characterized by suppressed firing rate for both the remember-first and remember-second tasks (Figures S3C-S3F). Firing rate was reduced not only in the fixation period but also in the visual stimulus presentation period and the delay period that followed it (Figures S3C and S3E). Firing rate remained at low levels when the visual stimuli to be remembered were presented out of the receptive field (Figures S3D and S3F). NB stimulation flattened the tuning curve of these neurons, too (Figure S3G).

DISCUSSION

Our behavioral results confirm recent studies that showed improvements in other cognitive tasks (Blake et al., 2017; Liu et al., 2017, 2018). Taken together, we have now shown working memory improvement by NB stimulation in two different cohorts of monkeys, tested in two different laboratories. Our neural results were generally consistent with the effects of cholinergic agonists, the iontophoresis of which increases activity of prefrontal neurons (Dasilva et al., 2019; Sun et al., 2017; Yang et al., 2013). Conversely, systemic administration of the muscarinic antagonist scopolamine (Zhou et al., 2011) and micro-iontophoresis of muscarinic and nicotinic-α7 inhibitors reduce prefrontal activity (Galvin et al., 2020; Major et al., 2015; Yang et al., 2013). In contrast with these reported drug effects, however, NB stimulation produced an increase that was specific only for some stimulus conditions, notably not affecting the neuron's preferred responses. NB stimulation was delivered in an intermittent pattern and also likely excited GABAergic neurons with ascending projections that are concurrently active with cholinergic neurons (Kim et al., 2015; Walker et al., 1989), which may have played a role in determining selectivity during NB stimulation.

Neural tuning implications

The pharmacological studies reviewed above generally suggested that the mechanism through which cholinergic action improves cognitive performance was sharpening of receptive fields, similarly to the effects of dopamine agonists, which at low doses ''sculpt'' neuronal activity to improve spatial selectivity (Vijayraghavan et al., 2007), because narrower tuning may result in more efficient coding (Fitzpatrick et al., 1997). Broader tuning has in fact been observed in pharmacological studies by cholinergic overstimulation with high doses of carbachol or M1R allosteric inhibitors administered iontopho-retically, which reduce prefrontal selectivity in the context of working memory tasks (Galvin et al., 2020; Major et al., 2018; Vijayraghavan et al., 2018). The effect was assumed to correspond to the descending section of an inverted-U function, representing a regimen over which cholinergic stimulation will impair performance. The effectiveness of drugs targeting other neurotransmitter systems is also often interpreted in terms of increased stimulus selectivity (Williams and Goldman-Rakic, 1995).

Sharper tuning is typically associated with increased performance for conditions in which decoding of the precise stimulus location is essential, as in discrimination tasks, after perceptual learning (Li et al., 2004; Raiguel et al., 2006; Sanayei et al., 2018; Yang and Maunsell, 2004). Theoretical studies have shown, however, that broader tuning curves can produce either worse or better performance depending on the task and noise conditions in the network (Butts and Goldman, 2006; Ma et al., 2006; Pouget et al., 1999; Zhang and Sejnowski, 1999). For conditions in which stimuli are highly discriminable and performance depends on the ability to filter distractors or other intervening noise and implement the correct rule, as was the case in our task, broader tuning of individual neurons may not necessarily lead to less efficient coding (Stein et al., 2021). Optimizing mechanisms to increase signal durability during delays may occur at a cost of the accuracy in the signal being carried, and a stability-accuracy tradeoff ends up determining overall performance in

a task. Unlike the effects of perceptual learning mentioned above, learning a spatial working memory task also induces broadening of neural selectivity in PFC (Qi et al., 2011). One existing class of models, the bump attractor model, enables exploration of the impact of broadened tuning on working memory accuracy (Compte et al., 2000; Wimmer et al., 2014). The network behaves as a continuous attractor (Seung et al., 2000), allowing activity to persist even when the original visual stimulus is no longer present but making the storage of parametric quantities sensitive to internal noise fluctuations. Whole-network modulation, such as by NB stimulation that results in a broader bump of activity, renders the network more resistant to noise fluctuations that perturb memory maintenance (Stein et al., 2021). The broadening of neuronal tuning is not without costs, however, and NB stimulation degraded performance when distractors were present in close proximity to the stimulus.

Areal effects

The effects of cholinergic agents in sensory areas are markedly different from those in the PFC. Agonist administration in the primary visual cortex enhances responses during visual stimulus presentation and for attended over unattended ones (Herrero et al., 2008). Similarly, cholinergic agonists and antagonists in area MT affect responses to visual stimuli (Veith et al., 2021). Optogenetic phasic stimulation of cholinergic neurons has also been shown to improve visual perceptual discrimination by increasing firing rate during the period of visual stimulus presentations (Pinto et al., 2013). Neuronal responses within the NB often signal novelty or surprise (Zhang et al., 2019), and widely distributed projections of these neurons appear to play different roles at different parts of the cortex. NB stimulation is likely to activate other areas of the association cortex, in addition to the PFC, including the posterior parietal cortex (Mesulam et al., 1983). Posterior parietal neurons exhibit persistent activity in similar tasks, and their activation by NB stimulation is consistent with both our experiment results and their known role in cognitive tasks (Riley and Constantinidis, 2016).

Stimulation parameters

Our protocol of NB stimulation can improve cognitive performance only when administered in an intermittent fashion, for 15–20 s/min (Liu et al., 2017). The result suggests that continuous stimulation may lead to depletion of acetylcholine reserves, a phenomenon consistent with the known impairment of working memory caused by acetylcholine depletion in the PFC (Croxson et al., 2011). Prolonged systemic administration of cholinergic agents may have a similar effect, which would account for its loss of effectiveness in patients with Alzheimer’s disease. The combination of judicious pattern of stimulation and recruitment of the full apparatus of ascending modulatory control appears to be critical for the success of cholinergic stimulation.

STAR ★METHODS

RESOURCE AVAILABILITY

Lead contact—Further information and requests for resources and reagents should be directed to and will be fulfilled by the Lead Contact, Dr. Christos Constantinidis (Christos.Constantinidis.1@vanderbilt.edu).

Materials availability—This study did not generate new unique reagents.

Data and code availability

- Data used for the analysis and figures have been deposited at Mendeley.com and are publicly available as of the date of publication. DOIs are listed in the Key resources table.
- This paper does not report original code
- Any additional information required to reanalyze the data reported in this paper is available from the lead contact upon request.

EXPERIMENTAL MODEL AND SUBJECT DETAILS

Two adult male, rhesus monkeys (*Macaca mulatta*) weighing 7-10 kg were used in this study. All experimental procedures followed guidelines by the U.S. Public Health Service Policy on Humane Care and Use of Laboratory Animals and the National Research Council's Guide for the Care and Use of Laboratory Animals and were reviewed and approved by the Wake Forest University Institutional Animal Care and Use Committee under protocol number A16-023. Animals were maintained in an AAALAC accredited facility managed by the Animal Resources Program of the Wake Forest University School of Medicine, which was housing several individuals of the same species.

METHOD DETAILS

Surgery and neurophysiology—A 20-mm-diameter recording cylinder was implanted over the dorsolateral prefrontal cortex (dlPFC - Figure 1). A second cylinder was also implanted over the PPC of each monkey at the same time, but this was not used in the current experiment. Extracellular activity of single units was recorded from areas 8a and 46 of dlPFC. The anatomic location of electrode penetrations was determined on the basis of MR imaging. Recordings were obtained with arrays of two to four microelectrodes in the cylinder. These were epoxylite-coated tungsten electrodes with a 250 μm diameter and 1-4 MΩ impedance at 1 kHz (FHC, Bowdoin, ME). The electrical signal from each electrode was amplified, band-pass filtered between 500 Hz and 8 kHz, and recorded with a modular data acquisition system at 25-μs resolution (APM system; FHC, Bowdoin, ME). Waveforms that exceeded a user-defined threshold were sampled at 25 μs resolution, digitized, and stored for offline analysis. LFP recordings were obtained from the same electrodes by splitting the signal, filtering between 0.5 Hz and 100 Hz, and acquiring data at a 500 Hz sampling rate.

Deep Brain Electrode Implantation and Stimulation—Once the head-cap and recording cylinders had been implanted, a second surgery was performed to implant the stimulating electrode. Based on MR imaging, stereotaxic coordinates were obtained for targeted implantation. The animals were implanted unilaterally (one in the left, and one in the right hemisphere) at 8 mm lateral, 16 mm anterior interaural, and 29 mm below the cortical surface in a vertical penetration. The lateral and anterior coordinates, and depth, were chosen to correspond to the center of the anterior portion of the Nucleus Basalis of Meynert, which would contain the highest density of projections to the prefrontal

cortex (Gielow and Zaborszky, 2017; Mesulam et al., 1983). A small cylindrical titanium chamber (5-mm inner diameter and 7-mm outer) was mounted on the cranium and chamber was encased in bone cement, in continuity with the existing head-cap. A 26 ga. sharp hypodermic guide tube was lowered and the tip advanced 5 mm below the dura mater. The stimulation electrode was inserted into the guide tube, and a stylus was used to push it to the appropriate depth. The guide tube was then raised while the stylus depth maintained. The chamber was evacuated of fluid, flushed with ceftriaxone, and thereafter fluid evacuated a second time. Silicone was poured into the chamber to seal the fenestrations in the skull and the inside of the chamber. The rear end of the electrode could be continuously visualized to confirm proper depth. The electrode was fixed in depth with a drop of cyanoacrylate. One week after the surgery, the animals returned to behavioral studies. Placement of the electrode was verified with CT scanning, after implantation, in one animal.

The stimulation pulses were created by an isolated pulse stimulator (Model 2100, A-M Systems, Sequim WA), which was controlled by custom programed software, written on the MATLAB platform Impedances of electrodes were checked monthly during experiments. Intermittent stimulation was applied for 15 s at 80 pulses per second, followed by approximately 45 s with no stimulation. Stimulation was applied in the inter-trial interval, after a trial had completed, and a new trial began after stimulation had elapsed.

Stimulation electrodes were custom manufactured in our laboratory based on published specifications (McCairn and Turner, 2009). Conductors were 50 μm Pt/Ir, Teflon-insulated wire (A-M systems, Seattle, WA) embedded within a 30 ga. hypodermic tube, which was encased in a 28 ga. polyimide sheath. The wire extended from the end of the sheath into the brain tissue by roughly 1 mm, and the last 0.7 mm of insulation was stripped to achieve impedances of 5-10 kOhm at 1 kHz. The far end of the electrode was soldered to an extracranial connector fixed on the chamber outer wall. Prior experiments on electrode placement tested the effects of short periods of stimulation on EEG desynchronization (Liu et al., 2017). Stimulation was delivered with biphasic, negative first, unipolar 200 μA pulses with 100 μs per phase, and 80 Hz pulses were delivered for 100 ms. This resulted in LFP desynchronization obtained through the stimulation electrode when the electrode was at a depth corresponding to the atlas position of Nucleus Basalis. In prior experiments, an electrode movement vertically in either direction of more than 1 mm was adequate to make desynchronization not possible using the same protocol (Liu et al., 2017). LFP recordings obtained through the stimulating electrode used the same filtering and sampling parameters as the recording electrodes (band pass filtering between 0.5 – 100 Hz, sampling at 500 Hz).

Behavioral tasks—The monkeys faced a computer monitor 60 cm away in a dark room with their head fixed. Eye position was sampled at 240 Hz, digitized, and recorded with an infrared eye position tracking system (model RK-716; ISCAN, Burlington, MA). The visual stimulus presentation and behavior monitoring were controlled by in-house software (Meyer and Constantinidis, 2005) implemented in the MATLAB computational environment (Mathworks, Natick, MA).

The tasks used in the present study were variations of the Oculomotor Delayed Response task, but involving two visual stimuli appearing in sequence, requiring the monkey to

remember and make an eye movement to the location of either the first or the second visual stimulus (Figure 2). The monkeys were trained to saccade to the location of the remembered visual stimulus according to the color of fixation point. After the animals fixated at a white/blue square (0.2° in size) located at the center of the monitor for 1 s, two white squares (1.5° in size, 125 cd/m^2 in luminance, 99% Michelson contrast) were displayed sequentially for 0.5 s, with a 1 s intervening delay period. The first visual stimulus was displayed at one of eight possible locations arranged along a circular ring of 12° eccentricity, with a 45° angular separation between neighboring visual stimuli. The monkeys were trained with stimulus appearances at every possible location, however, during recordings the first stimulus appeared at one of these eight locations and its diametric location. This was followed by a second visual stimulus, which was displaced 0, 45, 90, or 180° relative to the first. Two additional, “null” conditions were included, in which either the first or second stimulus presentation was omitted, so that there were 10 trial types in total, and these were used with equal frequency. After a second delay period of 1 s, the monkeys were required to saccade to the location of the first visual stimulus if the fixation point was white in color (remember-first condition), and to the location of the second visual stimulus if the fixation point was blue (remember-second condition). The monkeys were rewarded with juice after making a correct saccade. Deviating gaze beyond a 3°-radius fixation window led to the immediate termination of the trial without reward.

At the beginning of each recording session, we first ran the ODR task with a single stimulus, as a way to approximately map the receptive fields of neurons isolated from our electrodes. Then the remember-first and remember-second task began. To minimize the uncertainty about the visual stimulus to be remembered, the remember-first and remember-second conditions were presented in blocks of trials. The animal was required to perform ten correct trials of the remember-first task, before the task alternated to the remember-second condition. During sessions of NB stimulation that were delivered in block mode (trials with and without stimulation collected during the same daily session), approximately 60 trials were collected for each block, which therefore involved 6 alterations between the remember-first and remember-second rule.

Behavioral Performance—We calculated behavioral performance as the percentage of trials that resulted in correct saccades into the target window, a 7° circle around the center of the visual stimulus. Trials that were aborted prior to end of the second delay period (due to premature saccades, or blinks) were not included in this analysis. Performance in a single daily session was used as a unit of analysis in Figure 2. A daily session included approximately 120 trials.

Immunohistochemistry and Fluorescence Imaging—Free floating 50-μm sections of fixed monkey brain were stained with Anti-ChAT antibody (MilliporeSigma, MAB5270), Goat Anti-Mouse-Biotin-SP antibody (Jackson ImmunoResearch Laboratories, 115-067-003), Streptavidin-HRP (PerkinElmer, NEL750), and SuperGlo Green fluorescein tyramide (Fluorescent Solutions, FS101). Stained sections were mounted on slides and z stack images were collected at 10X and 20X magnification using a Zeiss AxioImager

microscope. The coronal section displayed in Figure 1C was corresponded to a plane approximately 16 mm anterior to the interaural line.

QUANTIFICATION AND STATISTICAL ANALYSIS

All data analysis was implemented with the MATLAB computational environment (R2012-2019, Mathworks, Natick, MA). Recorded spike waveforms were sorted into separate units using an automated cluster analysis relying on the KlustaKwik algorithm (Harris et al., 2000), which relied on principal component analysis of the waveforms. Mean firing rate was then determined in each task interval. Neurons responsive to the visual stimuli were identified, evidenced by a significant increase in firing rate in either the cue period or delay period relative to the baseline fixation period (paired-t test, evaluated at the 0.05 significance level). These neurons were used for most analyses in the main text, however analyses including all neurons were also performed. Neural data from correct trials were used only in these analyses. Units were identified as broad-action potential, Regular Spiking (RS) neurons or narrow-action potential, Fast Spiking (FS) neurons, based on the width of the action potential. This was defined as the duration between two positive phases of the waveform, using a criterion value of 0.55 ms, as described before (Qi et al., 2011).

We identified neurons with a significant excitatory or inhibitory effect of stimulation by comparing baseline firing rate during the fixation period between the control and stimulation conditions (evaluated with a t test at the $p < 0.05$ level). To study separately effects of stimulation on the remember-first and remember-second task, we compared firing rates across conditions by performing a 2-way ANOVA with factors tasks and stimulation. We repeated this 2-way ANOVA for other task intervals, including the visual stimulus presentation and delay period. In a similar fashion, a 3-way ANOVA was performed in order to determine the main effect of task, location of first visual stimulus, and location of second visual stimulus on firing rate. This analysis was performed in a time-resolved fashion, in successive 250 ms windows spanning the entire trial.

The Fano factor of a neuron's discharge rate (defined as the variance divided by the mean) was estimated in different task periods. Data for each neuron and condition were treated separately. Spike counts were computed in a 100-ms sliding window moving in 20-ms steps. The method computes the variance and mean of the spike count across trials and performs a regression of the variance to the mean (Qi and Constantinidis, 2012). This slope of this regression represents the Fano Factor reported here.

We quantified selectivity for different visual stimulus location using a Selectivity Index (SI) defined as (Max−Min)/(Max+Min) where Max and Min represent the firing rate corresponding to the best and worst stimulus location for each neuron, determined independently for the cue and delay periods, and calculated over the entire cue/delay period. SI values were also determined independently for the control and NB-stimulation conditions. Discriminability between visual stimulus conditions does not only depend on mean firing rates, on which SI depends, but also their variance. We therefore compared the full distributions of firing rates between the worst and best condition using a Receiver Operating Characteristic analysis. This was performed in a time-resolved fashion, in successive 250 ms windows. The Percentage of Explained Variance (PEV) analysis calculated the ratio Sum of

Squares between stimulus conditions to the total Sum of Squares. This was also performed in time-resolved fashion, using 500 ms windows.

The endpoint of saccades toward the targets were analyzed in correct trials. For each monkey and visual stimulus condition, the mean saccadic endpoint was calculated for the target location (using circular mean statistics). We then computed the angular deviation of the saccadic endpoint in every trial, relative to the mean saccadic endpoint for that condition. We applied the Kuiper two-sample test, a circular analog of Kolmogorov-Smirnov test, to compare the distributions of angular deviations around the mean, with and without stimulation.

Supplementary Material

Refer to Web version on PubMed Central for supplementary material.

ACKNOWLEDGMENTS

Research reported in this paper was supported by NIH grants R01 MH097695 and RF1 AG060754 to C.C. and D.T.B. A.I.V. was supported by VA grant I01 BX003890. D.B. and A.C. were supported by the Spanish Ministry of Science and Innovation and European Regional Development Fund (Ref: RTI2018-094190-B-I00) and by the CERCA Programme/Generalitat de Catalunya. We wish to thank James Daunais, Kristopher Bunting, Austin Lodish, Sihai Li, and Junda Zhu for technical help; Alvin Terry for guidance with the design of the study; and John Murray and Joost Maier for valuable comments on the manuscript. The contents of this publication do not represent the views of the VA or the US Government.

REFERENCES

Bakin JS, and Weinberger NM (1996). Induction of a physiological memory in the cerebral cortex by stimulation of the nucleus basalis. Proc. Natl. Acad. Sci. USA 93, 11219–11224. [PubMed: 8855336]

Ballinger EC, Ananth M, Talmage DA, and Role LW (2016). Basal Forebrain Cholinergic Circuits and Signaling in Cognition and Cognitive Decline. Neuron 91, 1199–1218. [PubMed: 27657448]

Birks JS, and Harvey RJ (2018). Donepezil for dementia due to Alzheimer's disease. Cochrane Database Syst. Rev 6, CD001190 [PubMed: 29923184]

Bjordahl TS, Dimyan MA, and Weinberger NM (1998). Induction of longterm receptive field plasticity in the auditory cortex of the waking guinea pig by stimulation of the nucleus basalis. Behav. Neurosci 112, 467–479. [PubMed: 9676965]

Blake DT, Terry AV, Plagenhoef M, Constantinidis C, and Liu R (2017). Potential for intermittent stimulation of nucleus basalis of Meynert to impact treatment of alzheimer's disease. Commun. Integr. Biol 10, e1389359. [PubMed: 29260798]

Brzosko Z, Mierau SB, and Paulsen O (2019). Neuromodulation of Spike-Timing-Dependent Plasticity: Past, Present, and Future. Neuron 103,563–581. [PubMed: 31437453]

Butts DA, and Goldman MS (2006). Tuning curves, neuronal variability, and sensory coding. PLoS Biol. 4, e92. [PubMed: 16529529]

Compte A, Brunel N, Goldman-Rakic PS, and Wang XJ (2000). Synaptic mechanisms and network dynamics underlying spatial working memory in a cortical network model. Cereb. Cortex 10, 910–923. [PubMed: 10982751]

Constantinidis C, and Klingberg T (2016). The neuroscience of working memory capacity and training. Nat. Rev. Neurosci 17, 438–449. [PubMed: 27225070]

Croxson PL, Kyriazis DA, and Baxter MG (2011). Cholinergic modulation of a specific memory function of prefrontal cortex. Nat. Neurosci 14, 1510–1512. [PubMed: 22057191]

Dasilva M, Brandt C, Gotthardt S, Gieselmann MA, Distler C, and Thiele A (2019). Cell class-specific modulation of attentional signals by acetylcholine in macaque frontal eye field. Proc. Natl. Acad. Sci. USA 116, 20180–20189. [PubMed: 31527242]

Fitzpatrick DC, Batra R, Stanford TR, and Kuwada S (1997). A neuronal population code for sound localization. Nature 388, 871–874. [PubMed: 9278047]

Freund HJ, Kuhn J, Lenartz D, Mai JK, Schnell T, Klosterkoetter J, and Sturm V (2009). Cognitive functions in a patient with Parkinson-dementia syndrome undergoing deep brain stimulation. Arch. Neurol 66, 781–785. [PubMed: 19506141]

Froemke RC (2015). Plasticity of cortical excitatory-inhibitory balance. Annu. Rev. Neurosci 38, 195–219. [PubMed: 25897875]

Galvin VC, Arnsten AFT, and Wang M (2018). Evolution in Neuromodulation-The Differential Roles of Acetylcholine in Higher Order Association vs. Primary Visual Cortices. Front. Neural Circuits 12, 67. [PubMed: 30210306]

Galvin VC, Yang ST, Paspalas CD, Yang Y, Jin LE, Datta D, Morozov YM, Lightbourne TC, Lowet AS, Rakic P, et al. (2020). Muscarinic M1 Receptors Modulate Working Memory Performance and Activity via KCNQ Potassium Channels in the Primate Prefrontal Cortex. Neuron 106, 649–661.e4. [PubMed: 32197063]

Gielow MR, and Zaborszky L (2017). The Input-Output Relationship of the Cholinergic Basal Forebrain. Cell Rep. 18, 1817–1830. [PubMed: 28199851]

Harris KD, Henze DA, Csicsvari J, Hirase H, and Buzsáki G (2000). Accuracy of tetrode spike separation as determined by simultaneous intracellular and extracellular measurements. J. Neurophysiol 84, 401–414. [PubMed: 10899214]

Herrero JL, Roberts MJ, Delicato LS, Gieselmann MA, Dayan P, and Thiele A (2008). Acetylcholine contributes through muscarinic receptors to attentional modulation in V1. Nature 454, 1110–1114. [PubMed: 18633352]

Kilgard MP, and Merzenich MM (1998). Cortical map reorganization enabled by nucleus basalis activity. Science 279, 1714–1718. [PubMed: 9497289]

Kim T, Thankachan S, McKenna JT, McNally JM, Yang C, Choi JH, Chen L, Kocsis B, Deisseroth K, Strecker RE, et al. (2015). Cortically projecting basal forebrain parvalbumin neurons regulate cortical gamma band oscillations. Proc. Natl. Acad. Sci. USA 112, 3535–3540. [PubMed: 25733878]

Li W, Piëch V, and Gilbert CD (2004). Perceptual learning and top-down influences in primary visual cortex. Nat. Neurosci 7, 651–657. [PubMed: 15156149]

Liu R, Crawford J, Callahan PM, Terry AV Jr., Constantinidis C, and Blake DT (2017). Intermittent Stimulation of the Nucleus Basalis of Meynert Improves Working Memory in Adult Monkeys. Curr. Biol 27, 2640–2646.e4. [PubMed: 28823679]

Liu R, Crawford J, Callahan PM, Terry AV, Constantinidis C, and Blake DT (2018). Intermittent stimulation in the nucleus basalis of meynert improves sustained attention in rhesus monkeys. Neuropharmacology 137, 202–210. [PubMed: 29704983]

Ma WJ, Beck JM, Latham PE, and Pouget A (2006). Bayesian inference with probabilistic population codes. Nat. Neurosci 9, 1432–1438. [PubMed: 17057707]

Major AJ, Vijayraghavan S, and Everling S (2015). Muscarinic Attenuation of Mnemonic Rule Representation in Macaque Dorsolateral Prefrontal Cortex during a Pro- and Anti-Saccade Task. J. Neurosci 35, 16064–16076. [PubMed: 26658860]

Major AJ, Vijayraghavan S, and Everling S (2018). Cholinergic Overstimulation Attenuates Rule Selectivity in Macaque Prefrontal Cortex. J. Neurosci 38, 1137–1150. [PubMed: 29255006]

McCairn KW, and Turner RS (2009). Deep brain stimulation of the globus pallidus internus in the parkinsonian primate: local entrainment and suppression of low-frequency oscillations. J. Neurophysiol 101, 1941–1960. [PubMed: 19164104]

Mesulam MM, Mufson EJ, Levey AI, and Wainer BH (1983). Cholinergic innervation of cortex by the basal forebrain: cytochemistry and cortical connections of the septal area, diagonal band nuclei, nucleus basalis (substantia innominata), and hypothalamus in the rhesus monkey. J. Comp. Neurol 214, 170–197. [PubMed: 6841683]

Meyer T, and Constantinidis C (2005). A software solution for the control of visual behavioral experimentation. J. Neurosci. Methods 142, 27–34. [PubMed: 15652614]

Pinto L, Goard MJ, Estandian D, Xu M, Kwan AC, Lee SH, Harrison TC, Feng G, and Dan Y (2013). Fast modulation of visual perception by basal forebrain cholinergic neurons. Nat. Neurosci 16, 1857–1863. [PubMed: 24162654]

Pouget A, Deneve S, Ducom JC, and Latham PE (1999). Narrow versus wide tuning curves: What's best for a population code? Neural Comput. 11, 85–90. [PubMed: 9950723]

Qi XL, and Constantinidis C (2012). Variability of prefrontal neuronal discharges before and after training in a working memory task. PLoS ONE 7, e41053. [PubMed: 22848426]

Qi XL, Meyer T, Stanford TR, and Constantinidis C (2011). Changes in prefrontal neuronal activity after learning to perform a spatial working memory task. Cereb. Cortex 21, 2722–2732. [PubMed: 21527786]

Raiguel S, Vogels R, Mysore SG, and Orban GA (2006). Learning to see the difference specifically alters the most informative V4 neurons. J. Neurosci 26, 6589–6602. [PubMed: 16775147]

Riley MR, and Constantinidis C (2016). Role of prefrontal persistent activity in working memory. Front. Syst. Neurosci 9, 181. [PubMed: 26778980]

Sanayei M, Chen X, Chicharro D, Distler C, Panzeri S, and Thiele A (2018). Perceptual learning of fine contrast discrimination changes neuronal tuning and population coding in macaque V4. Nat. Commun 9, 4238. [PubMed: 30315163]

Sarter M, Lustig C, Berry AS, Gritton H, Howe WM, and Parikh V (2016). What do phasic cholinergic signals do? Neurobiol. Learn. Mem 130, 135–141. [PubMed: 26911787]

Seung HS, Lee DD, Reis BY, and Tank DW (2000). Stability of the memory of eye position in a recurrent network of conductance-based model neurons. Neuron 26, 259–271. [PubMed: 10798409]

Stein H, Barbosa J, and Compte A (2021). Towards biologically constrained attractor models of schizophrenia. PsyArXiv. 10.31234/osf.io/uxg2a.

Sun Y, Yang Y, Galvin VC, Yang S, Arnsten AF, and Wang M (2017). Nicotinic α4β2 Cholinergic Receptor Influences on Dorsolateral Prefrontal Cortical Neuronal Firing during a Working Memory Task. J. Neurosci 37, 5366–5377. [PubMed: 28450546]

Terry AV Jr., and Buccafusco JJ (2003). The cholinergic hypothesis of age and Alzheimer's disease-related cognitive deficits: recent challenges and their implications for novel drug development. J. Pharmacol. Exp. Ther 306, 821–827. [PubMed: 12805474]

Veith VK, Quigley C, and Treue S (2021). Cholinergic manipulations affect sensory responses but not attentional enhancement in macaque MT. BMC Biol. 19, 49. [PubMed: 33726757]

Vijayraghavan S, Wang M, Birnbaum SG, Williams GV, and Arnsten AF (2007). Inverted-U dopamine D1 receptor actions on prefrontal neurons engaged in working memory. Nat. Neurosci 10, 376–384. [PubMed: 17277774]

Vijayraghavan S, Major AJ, and Everling S (2018). Muscarinic M1 Receptor Overstimulation Disrupts Working Memory Activity for Rules in Primate Prefrontal Cortex. Neuron 98, 1256–1268.e4. [PubMed: 29887340]

Walker LC, Price DL, and Young WS 3rd. (1989). GABAergic neurons in the primate basal forebrain magnocellular complex. Brain Res. 499,188–192. [PubMed: 2804667]

Williams GV, and Goldman-Rakic PS (1995). Modulation of memory fields by dopamine D1 receptors in prefrontal cortex. Nature 376, 572–575. [PubMed: 7637804]

Wimmer K, Nykamp DQ, Constantinidis C, and Compte A (2014). Bump attractor dynamics in prefrontal cortex explains behavioral precision in spatial working memory. Nat. Neurosci 17, 431–439. [PubMed: 24487232]

Yang T, and Maunsell JH (2004). The effect of perceptual learning on neuronal responses in monkey visual area V4. J. Neurosci 24, 1617–1626. [PubMed: 14973244]

Yang Y, Paspalas CD, Jin LE, Picciotto MR, Arnsten AF, and Wang M(2013). Nicotinic α7 receptors enhance NMDA cognitive circuits in dorsolateral prefrontal cortex. Proc. Natl. Acad. Sci. USA110, 12078–12083. [PubMed: 23818597]

Yuan R, Biswal BB, and Zaborszky L (2019). Functional Subdivisions of Magnocellular Cell Groups in Human Basal Forebrain: Test-Retest Resting-State Study at Ultra-high Field, and Meta-analysis. Cereb. Cortex 29, 2844–2858. [PubMed: 30137295]

Zhang K, and Sejnowski TJ (1999). Neuronal tuning: To sharpen or broaden? Neural Comput. 11, 75–84. [PubMed: 9950722]

Zhang K, Chen CD, and Monosov IE (2019). Novelty, Salience, and Surprise Timing Are Signaled by Neurons in the Basal Forebrain. Curr. Biol 29, 134–142.e3. [PubMed: 30581022]

Zhou X, Qi XL, Douglas K, Palaninathan K, Kang HS, Buccafusco JJ, Blake DT, and Constantinidis C (2011). Cholinergic modulation of working memory activity in primate prefrontal cortex. J. Neurophysiol 106,2180–2188. [PubMed: 21795623]

Highlights

- Monkey performance of working memory tasks improves with nucleus basalis (NB) stimulation
- Activity of prefrontal neurons increases under NB stimulation
- Tuning of neurons becomes broader, making the network more stable
- Working memory performance is determined by a stability-accuracy tradeoff

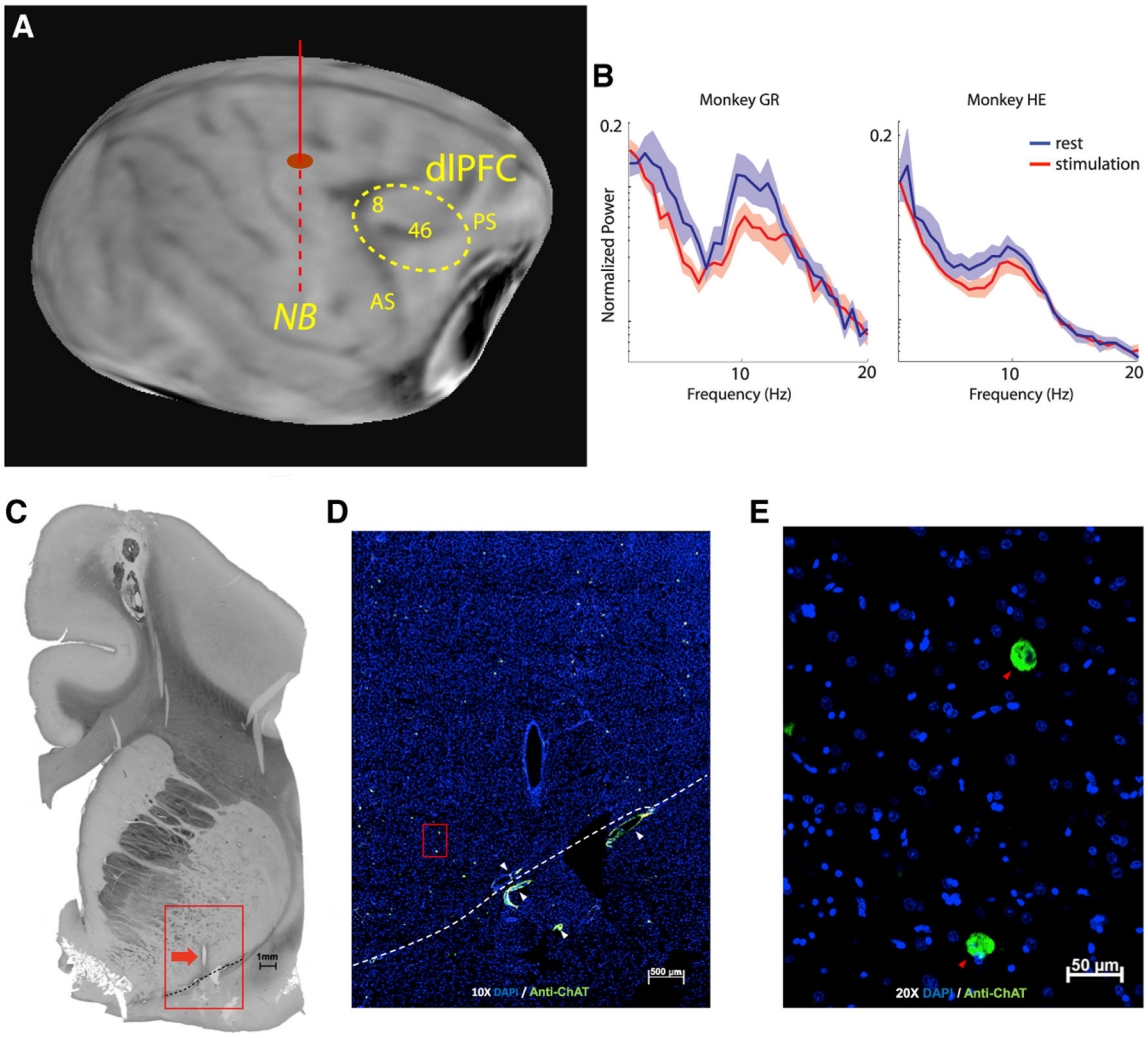

Figure 1. Localization and effects of stimulation

(A) Anatomical MR scan obtained prior to implantation. The approximate location of the implanted electrode is indicated with the solid/dashed vertical line. The dotted area represents the cortical region sampled with neurophysiological recordings.

(B) Power spectrum of local field potential recorded from the implanted electrode during rest and following 80-Hz stimulation in the two animals (subject HE, n = 34 spectra; subject GR, n = 18 spectra). Shaded area represents SEM.

(C) Histology and ChAT immunohistochemistry. A 50-µm-thick coronal plane section is viewed in light microscopy displaying the most inferior track of the electrode cannula. The red box surrounds the cannula track (red arrow) and indicates the area enlarged in (D). The dashed line marks the floor of the nucleus basalis. Scale bar: 1 mm.

(D) The marked area enlarged shown under merged green and blue fluorescence. Blue color marks nuclei with DAPI, and green marks antibody to ChAT. White arrowheads mark blood vessel autofluorescence. The dashed line is the same as in (A) and marks the floor of the basal forebrain. Scale bar: 500 µm.

(E) Nucleus basalis at 20x original magnification. DAPI (blue), anti-ChAT (green), and anti-ChAT-containing neurons (red arrowheads). Scale bar: 50 μm.
AS, arcuate sulcus; PS, principal sulcus.

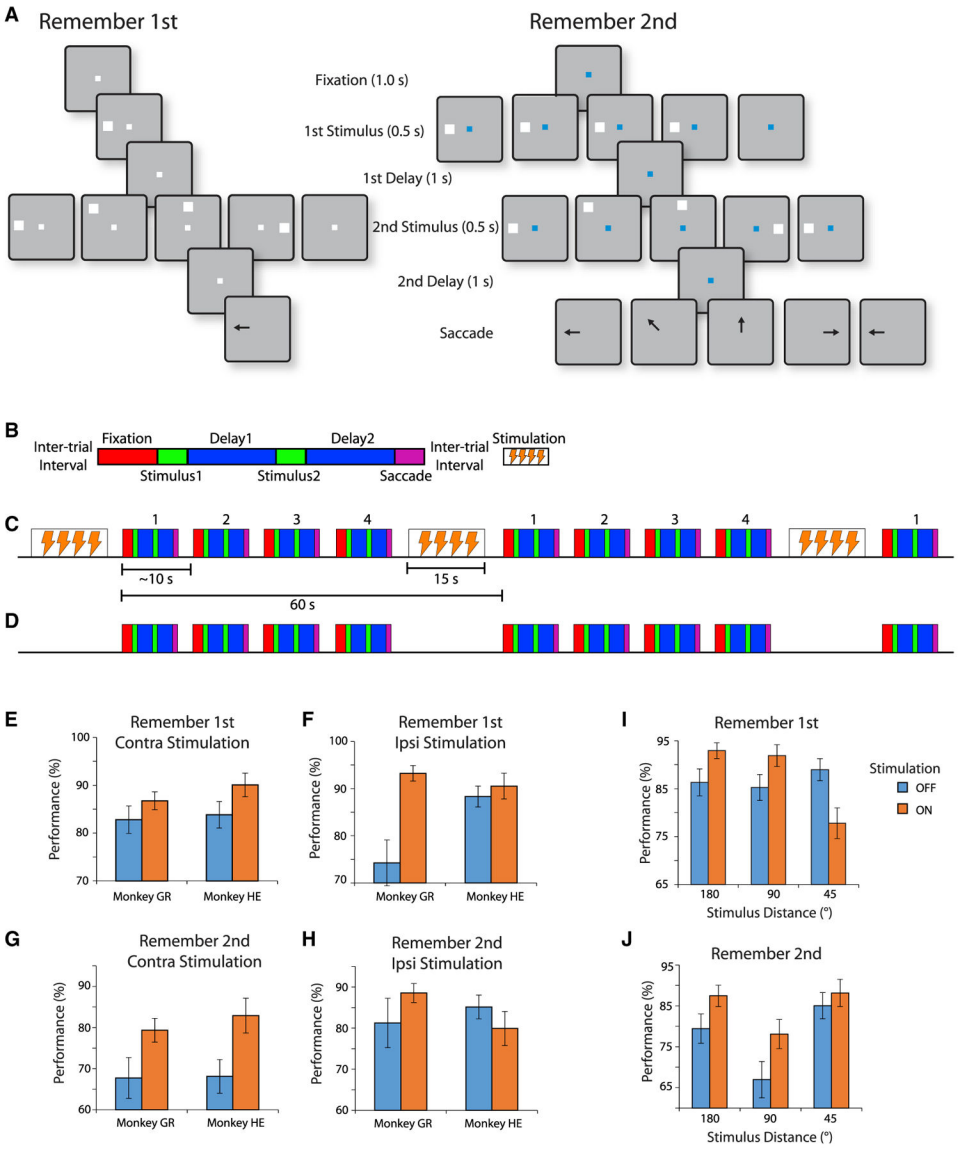

Figure 2. Behavioral task and performance

(A) Successive frames illustrate the sequence of events in the behavioral task. Depending on the white or blue color of the fixation point, the monkey has to remember either the first or the second of two visual stimuli presented in sequence, respectively. At the end of the trial, the fixation point turns off, and the monkey needs to perform an eye movement toward the remembered location of the visual stimulus in order to receive a liquid reward.

(B) Schematic diagram of a single trial of the task. Blocks represent the successive events in the task: fixation, first visual stimulus presentation, first delay period, second visual stimulus presentation, second delay period, and saccade. Successive trials are separated by inter-trial intervals. NB stimulation, when delivered, always occurs during the inter-trial interval.

(C) Sequence of trials during a stimulation block, in a compressed timescale, relative to (B). Successive trials, labeled 1–4, each lasting approximately 10 s, are followed by 15 s of stimulation. The precise duration of a trial differed depending on how quickly the animal

initiated the trial and if the trial was successfully completed or aborted, e.g., due to a break in fixation.

(D) Sequence of trials during a control (no-stimulation) block. The trials are arranged exactly in the same fashion as in the stimulation block, including an extended inter-trial interval every 60 s, during which, however, no stimulation is applied (sham).

(E-H) Percentage of correct trials is shown for each of the two monkeys, for different visual stimulus types, under control conditions (blue bars) and under NB stimulation (orange bars). n = 18 sessions for stimulation and 17 for control for monkey GR; n = 19 for stimulation and 35 for control for monkey HE. (E) Mean performance for trials in which first visual stimulus appears contralateral to the stimulation site, when the monkey is executing the remember-first task and needs to remember the first visual stimulus. (F) Performance in the remember-first task when the first visual stimulus appears ipsilateral to the stimulation site. (G) Performance in the remember-second task, when the second visual stimulus appears contralateral to the stimulation site. (H) Performance in the remember-second task, when the second visual stimulus appears ipsilateral to the stimulation site.

(I) Performance in the remember-first task, for trials grouped by distance between the first and second visual stimulus (180°, 90°, or 45°), under stimulation or control conditions. Data from both monkeys are pooled together.

(J) Performance in the remember-second task, for trials grouped by distance. Error bars represent SEM in all panels.

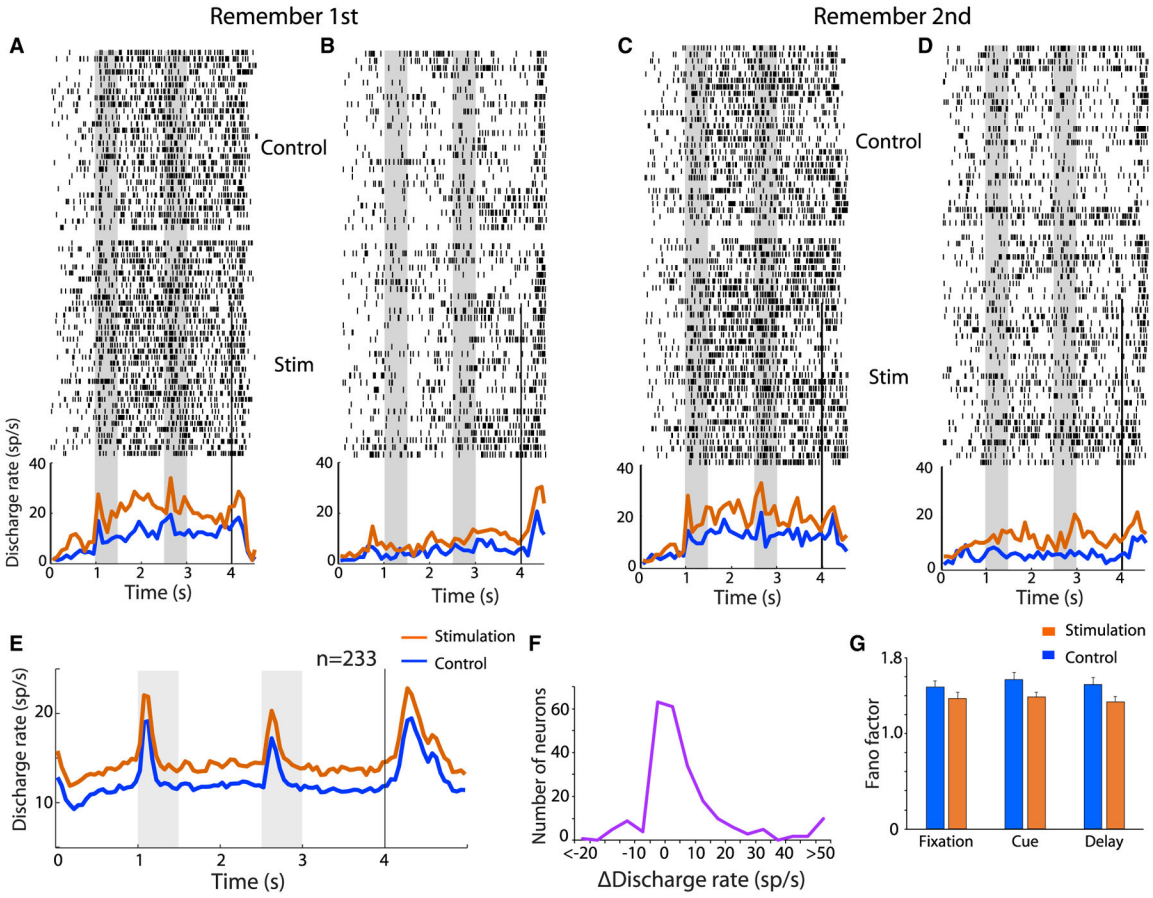

Figure 3. Neuronal stimulation effects

(A-D) Raster plots represent responses of a single prefrontal neuron in the remember-first (A and B) and remember-second tasks (C and D), under control and NB stimulation conditions. Line traces represent averaged, peri-stimulus time histograms, with and without NB stimulation. Trials are pooled from conditions when the first visual stimulus appeared to the contralateral (A and C) or ipsilateral hemifield (B and D). Gray bars indicate time of visual stimulus presentation.

(E) Population Peri-Stimulus Time Histogram (PSTH) averaged across all neurons (n = 233) and all stimulus conditions.

(F) Distribution of changes in firing rate in the fixation period across all neurons (n = 233).

(G) Mean Fano factor of spike counts averaged over the fixation, cue, and first delay period of the task (n = 233). Error bars represent SEM.

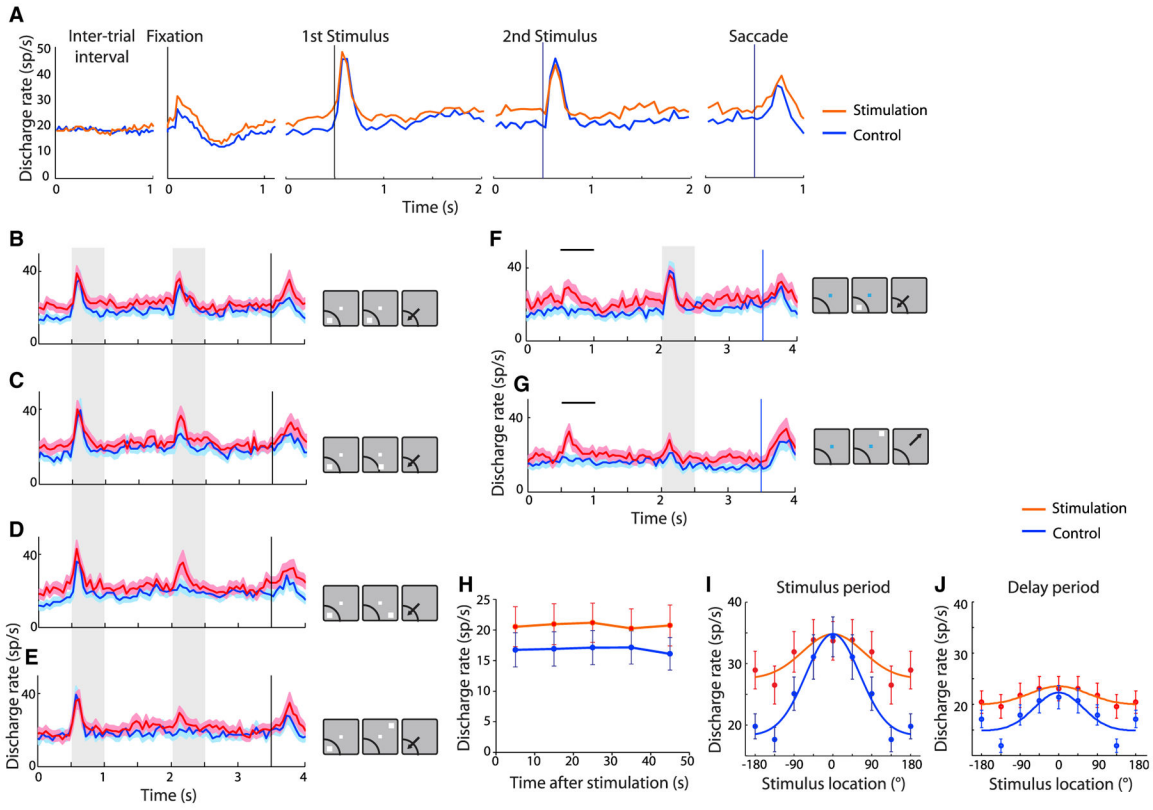

Figure 4. Task responses under stimulation

(A) Mean firing rate across neurons with and without NB stimulation is shown during the inter-trial interval, fixation interval, first visual stimulus presentation involving the best visual stimulus of each neuron, second visual stimulus presentation involving the best visual stimulus of each neuron, and saccade toward best visual stimulus. Results from the remember-second task are shown for neurons with significant increase in activation by NB stimulation (n = 54 neurons for all panels).

(B-E) Mean firing rate across neurons in the remember-first task, in conditions involving presentation of the first visual stimulus in the receptive field, followed by a second visual stimulus at progressively less responsive locations. Gray bars represent the times of visual stimulus presentations. Insets to the right of PSTH represent location of the visual stimuli relative to each neuron's receptive field; the receptive field is shown always at the same location for simplicity; results from neurons with different receptive field locations have been averaged together. Shaded area represents SEM.

(F and G) Mean firing rate across neurons in the remember-second task, in conditions involving no first visual stimulus, followed by a second visual stimulus in or out of the receptive field. Horizontal lines illustrate the times that a first visual stimulus would have been delivered relative to the onset of the fixation point, had one been present in these trials. Shaded area represents SEM.

(H) Firing rate in sequential trials in blocks of trials when stimulation was applied or not. Abscissa represents time after the offset of stimulation or sham inter-trial interval.

(I) Population tuning curve for the cue period, obtained by averaging responses of individual neurons to visual stimuli relative to each neuron's preferred reference location (depicted at 0°).

(J) As in (I), for the delay period. Error bars represent SEM.

KEY RESOURCES TABLE

REAGENT or RESOURCE	SOURCE	IDENTIFIER
Antibodies		
Anti-ChAT antibody	MilliporeSigma	MAB5270
Goat Anti-Mouse-Biotin-SP antibody	Jackson ImmunoResearch Laboratories	115–067-003
Chemicals, peptides, and recombinant proteins		
Streptavidin-HRP	PerkinElmer	NEL750
SuperGlo Green fluorescein tyramide	Fluorescent Solutions	FS101
Deposited data		
Figure data	This paper	https://dx.doi.org/10.17632/f9p96z597v.2
Experimental models: Organisms/strains		
Rhesus macaques (Macaca mulatta)	Alpha Genesis	N/A
Software and algorithms		
MATLAB	MathWorks	R2012–2019a
Other		
Microelectrodes	FHC	UEWLGGSE4N1E